Supporting information for

Cascades of Energy and Electron Transfer in a Panchromatic Absorber.

Jan Joseph,[a] Stefan Bauroth,[a] Asterios Charissiadis,[b] Georgios Charalambidis,[b] Athanassios G. Coutsolelos,[b,c] Dirk M. Guldi.[a]

[a]Department of Chemistry and Pharmacy and Interdisciplinary Center for Molecular Materials, Friedrich-Alexander-Universität, 91058 Erlangen, Germany.

[b]Department of Chemistry, University of Crete, Laboratory of Bioinorganic Chemistry, Voutes Campus, P.O. Box 2208, 71003 Heraklion, Crete, Greece.

[c]*Institute of Electronic Structure and Laser (IESL)Foundation for Research and Technology - Hellas (FORTH), Vassilika Vouton, GR 70013 Heraklion, Crete, Greece*

Contents

1.	Experimental section	2
2.	Electrochemistry	3
3.	Absorption and emission spectroscopy	4
4.	Transient absorption spectroscopy	5

Chemicals. Solvents (HPLC grade) were purchased from Sigma-Aldrich and Carl Roth and used as received without further purification.

Synthesis. BDP[1], **ZnP**[2] and **C_{60}**[3] were synthesized using a previously reported procedure.

Spectroscopy. UV/Vis absorption measurements at room temperature were performed in a 10x10 mm cuvette with a Lambda 2 double beam instrument (Perkin-Elmer). Fluorescence measurements were performed in a 10x10 mm cuvette with a Fluoromax 3 spectrometer (HORIBA Yobin).

Time-resolved absorption measurements were performed by using a Clark MXR CPA 2101 and CPA 2110 Ti:sapphire amplifier (775 nm, 1 kHz, 150 fs pulse width) as the laser source. Femtosecond transient absorption spectra were obtained by using an Ultrafast System HELIOS spectrometer with 150 fs resolution and time delays between 0 to 5500 ps. By focusing a fraction of the fundamental 775 nm onto a 2 mm sapphire disc the probe-visible white light (~400-770 nm) was generated. The probe-(near)IR light (780-1300 nm) was generated using a 1 cm sapphire disc. The excitation wavelengths of 430 and 505 nm were generated using a non-collinear optical parametric amplifier (NOPA, Clark MXR). A long-pass filter was used to exclude the fundamental 775 nm. Nanosecond transient absorption spectra were obtained by using an Ultrafast System EOS spectrometer with ~1 ns resolution and time delays between 0 to 400 µs. A built-in photonic crystal fiber supercontinuum laser source with a fundamental of 1064 nm at 2 kHz output frequency and pulse width of ~1 ns was used to generate the white light (~370 nm to >1600 nm). All measurements were performed in a 2 mm quartz cuvette under argon atmosphere at room temperature, with argon saturated anisole as solvent.

Electrochemistry. Differential pulse voltammetry (DPV) studies were performed with an Autolab PGSTAT101 potentiostat. Degassed DCM (bubbled with argon for 20 min) was used as solvent and 0.1 M tetra-n-butylammonium hexafluorophosphate (n-Bu_4NPF_6) as supporting electrolyte. A glassy carbon electrode was used as the working electrode, a platinum wire as the counter electrode and a Ag-wire as quasi-reference electrode. All potentials were corrected against the Fc+/Fc redox couple.

For spectroelectrochemical measurements a Metrohm PGSTAT101 potentiostat was used in combination with a Specord S600 UV/Vis spectrophotometer (Analytic Jena) in a home-built three-neck cell. To allow light passing through the sample solution, the used working electrode was a close meshed platinum net. A Ag-wire was used as reference electrode and a platinum wire was used as counter electrode. Degassed DCM (bubbled with argon for 20 min) was used as solvent and 0.1 M tetra-n-butylammonium hexafluorophosphate (n-Bu_4NPF_6) as supporting electrolyte.

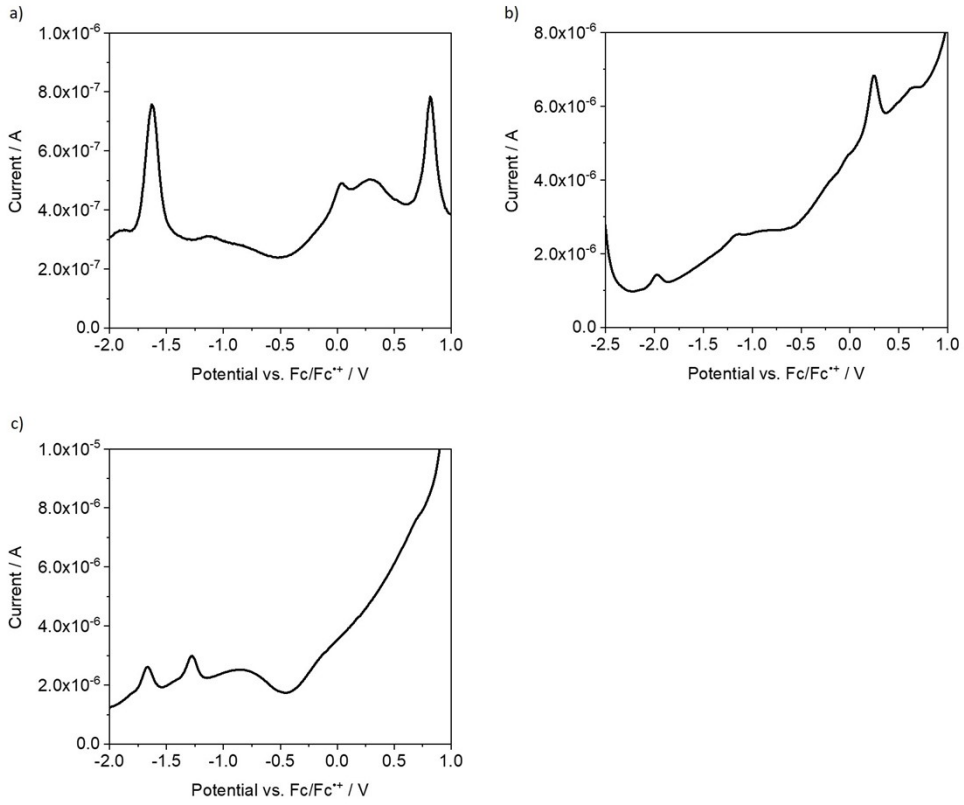

Fig. S1 Differential pulse voltammetry of a) **BDP**, b) **ZnP** and c) $\mathbf{C_{60}}$ in argon saturated DCM using 0.1 M $TBAPF_6$ as supporting electrolyte. A glassy carbon electrode was used as the working electrode, a platinum wire as the counter electrode and a Ag-wire as quasi-reference electrode.

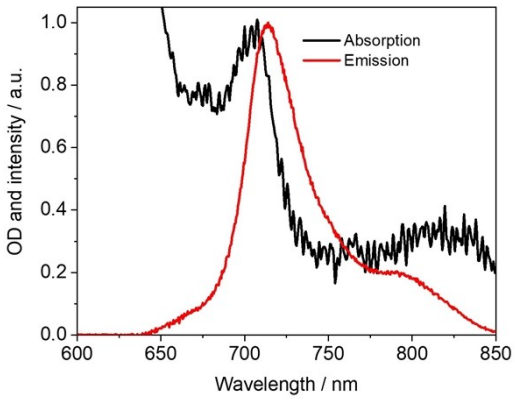

Fig. S2 Normalized absorption (black) and fluorescence spectrum (red) of $\mathbf{C_{60}}$ (c = 5.0 x 10^{-6} M, λ_{exc} = 320 nm) in anisole.

Merging of femto- and nanosecond transient absorption data:

Each set of femto- (HELIOS) and nanosecond (EOS) raw data was first prepared by the data analysis software “Surface Xplorer” (Ultrafast Systems): Light scattering correction (only EOS), chirp correction and t_0 correction. The processed data was then imported into Origin 2019 (OriginLab) and interpolated, to yield an equally distributed 0.5 nm interval for HELIOS and EOS data sets. Merging of HELIOS and EOS was done separately at each wavelength with the following equation in Excel (Microsoft):

$$OD_{HELIOS} = OD_{HELIOS,t} + \left(OD_{EOS,t,\,cut} - OD_{HELIOS,t,\,cut}\right)$$

The time delay, at which HELIOS was cut off and connected to EOS ($^{OD_{t,\,cut}}$), was chosen according to the best match of kinetics, i.e. 260 ps at 430 nm excitation and 3000 ps at 505 nm excitation. This procedure yielded the best results, because the global shape of each kinetic is preserved and lifetimes are not affected. As seen in the equation, only HELIOS data sets were modified this way. Therefore, only early species can show altered spectral features (e.g. ^{S1}**ZnP|C$_{60}$** in Fig. 10) due to adding or subtracting information from EOS to HELIOS in the merging process. This had, however, little to no impact on the quality and validity of the applied mechanistic models.

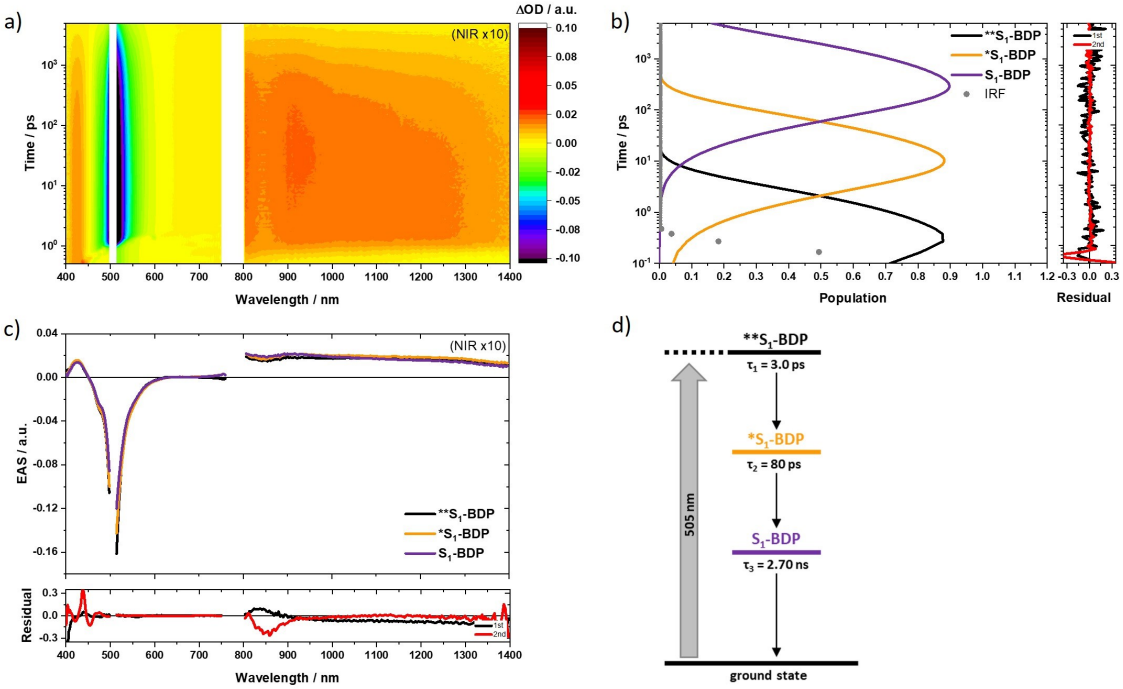

Fig. S3 a) Differential absorption spectra obtained upon femtosecond pump-probe experiments (505 nm) of a solution containing **BDP** (c = 4 x 10^{-5} M) in anisole with several time delays between 0.5 and 5500 ps. b) Population over time and c) SAS obtained upon chirp corrected GloTarAn analysis of the raw data with **$^{**}S_1$-BDP** (black), **$^{*}S_1$-BDP** (yellow), **S_1-BDP** (purple), IRF (circle), and corresponding first (black) and second (red) singular vectors of the residual on the right (for b) and bottom (for c). d) Mechanistic model applied in GloTarAn. Relative energies are arbitrary in favor of clarity.

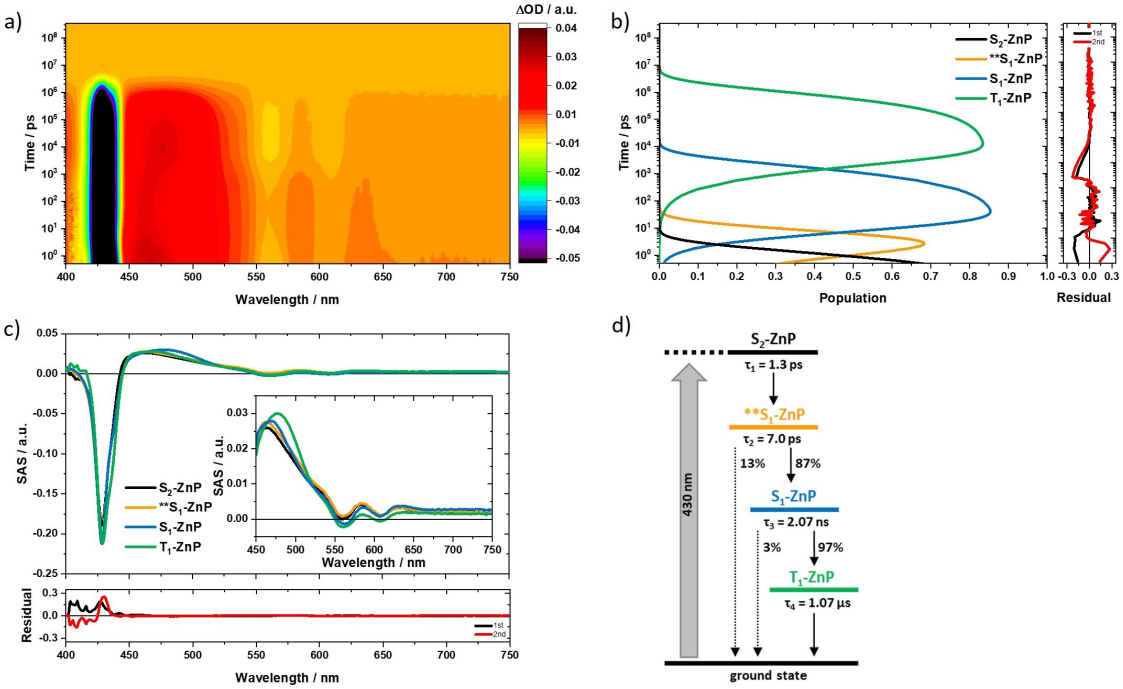

Fig. S4 a) Differential absorption spectra obtained upon combined femto- and nanosecond pump-probe experiments (430 nm) of a solution containing **ZnP** (c = 1 x 10^{-5} M) in anisole with several time delays between 0.5 and 400 µs. b) Population over time and c) SAS obtained upon GloTarAn analysis of the raw data with **S_2-ZnP** (black), ****S_1-ZnP** (yellow), **S_1-ZnP** (blue) and **T_1-ZnP** (green), and corresponding first (black) and second (red) singular vectors of the residual on the right (for b) and bottom (for c). d) Mechanistic model applied in GloTarAn. Relative energies are arbitrary in favor of clarity.

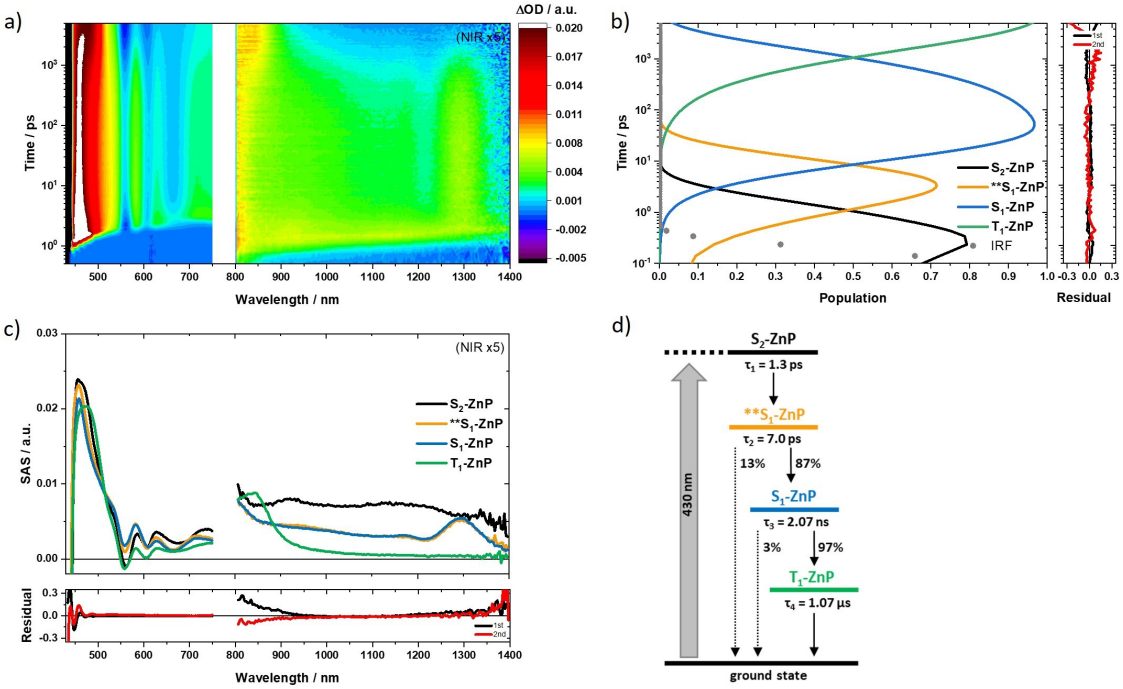

Fig. S5 a) Differential absorption spectra obtained upon femtosecond pump-probe experiments (430 nm) of a solution containing **ZnP** (c = 1 x 10^{-5} M) in anisole with several time delays between 0.5 and 5500 ps. b) Population over time and c) SAS obtained upon chirp corrected GloTarAn analysis of the raw data with **S_2-ZnP** (black), ****S_1-ZnP** (yellow), **S_1-ZnP** (blue) and **T_1-ZnP** (green), IRF (circle), and corresponding first (black) and second (red) singular vectors of the residual on the right (for b) and bottom (for c). d) Mechanistic model applied in GloTarAn. Relative energies are arbitrary in favor of clarity.

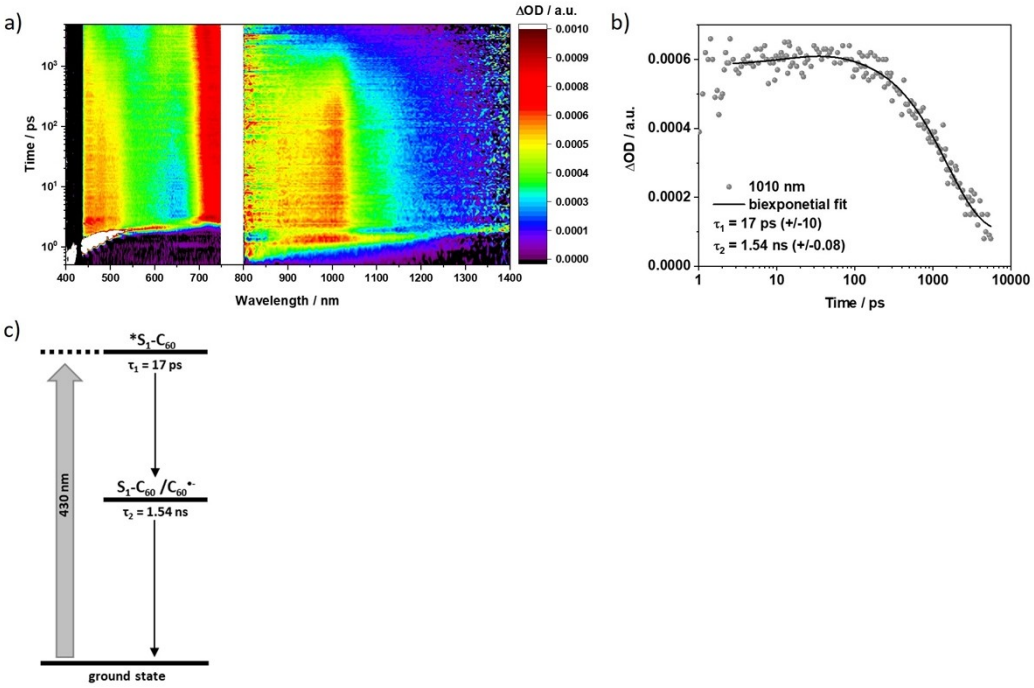

Fig. S6 a) Differential absorption spectra obtained upon femtosecond pump-probe experiments (430 nm) of a solution containing **C_{60}** (c = 4 x 10^{-5} M) in anisole with several time delays between 0.5 and 5500 ps. b) Absorption profile over time at 1010 nm (grey dots) and corresponding biexponential fit (black line). d) Corresponding deactivation pathway derived from the 1010 nm biexponential fit. Relative energies are arbitrary in favor of clarity.

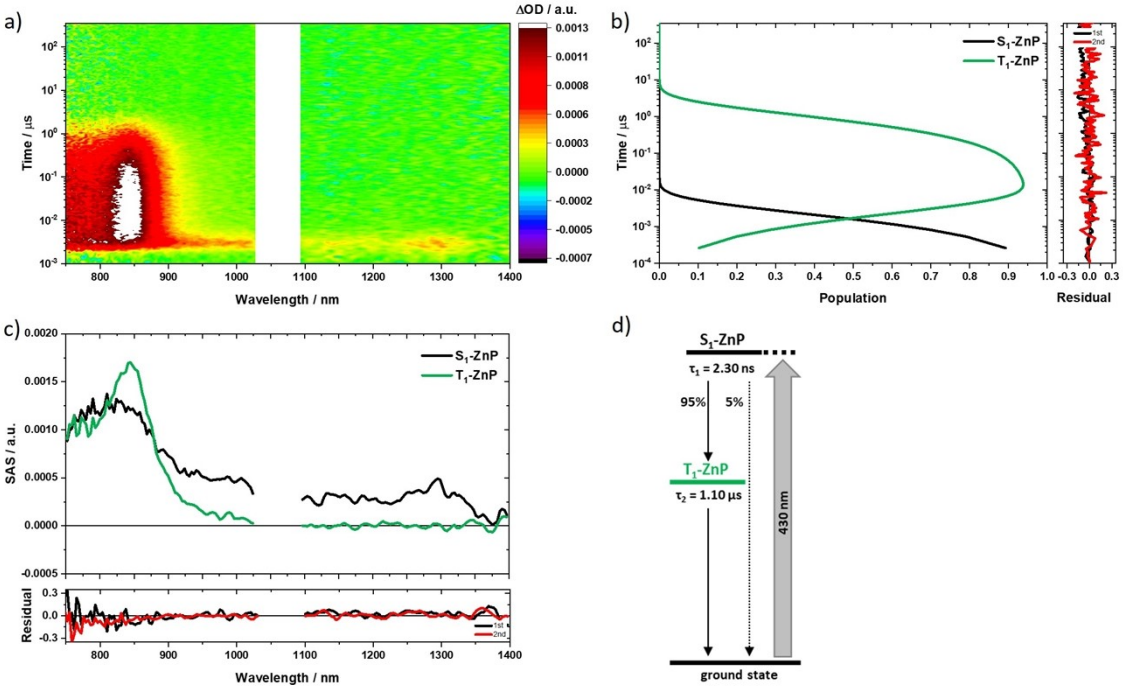

Fig. S7 a) Differential absorption spectra obtained upon nanosecond pump-probe experiments (430 nm) of a solution containing **ZnP** (c = 1 x 10^{-5} M) in anisole with several time delays between 0 and 400 µs. b) Population over time and c) SAS obtained upon chirp corrected GloTarAn analysis of the raw data with **S_1-ZnP** (black), **T_1-ZnP** (green), and corresponding first (black) and second (red) singular vectors of the residual on the right (for b) and bottom (for c). d) Mechanistic model applied in GloTarAn. Relative energies are arbitrary in favor of clarity.

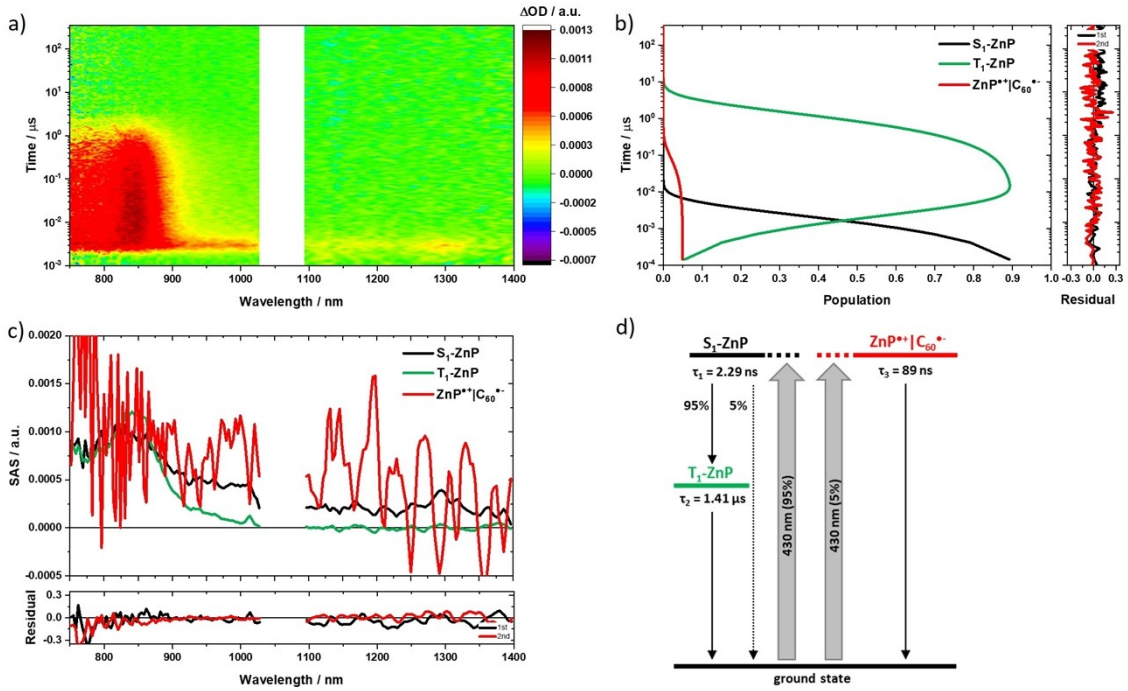

Fig. S8 a) Differential absorption spectra obtained upon nanosecond pump-probe experiments (430 nm) of a solution containing **ZnP** (c = 1 x 10^{-5} M) and $\mathbf{C_{60}}$ (c = 1 x 10^{-5} M) in anisole with several time delays between 0 and 400 µs. b) Population over time and c) SAS obtained upon chirp corrected GloTarAn analysis of the raw data with $\mathbf{S_1}$**-ZnP** (black), $\mathbf{T_1}$**-ZnP** (green), $\mathbf{ZnP^{\bullet+}|C_{60}^{\bullet-}}$ (red), and corresponding first (black) and second (red) singular vectors of the residual on the right (for b) and bottom (for c). d) Mechanistic model applied in GloTarAn. Relative energies are arbitrary in favor of clarity.

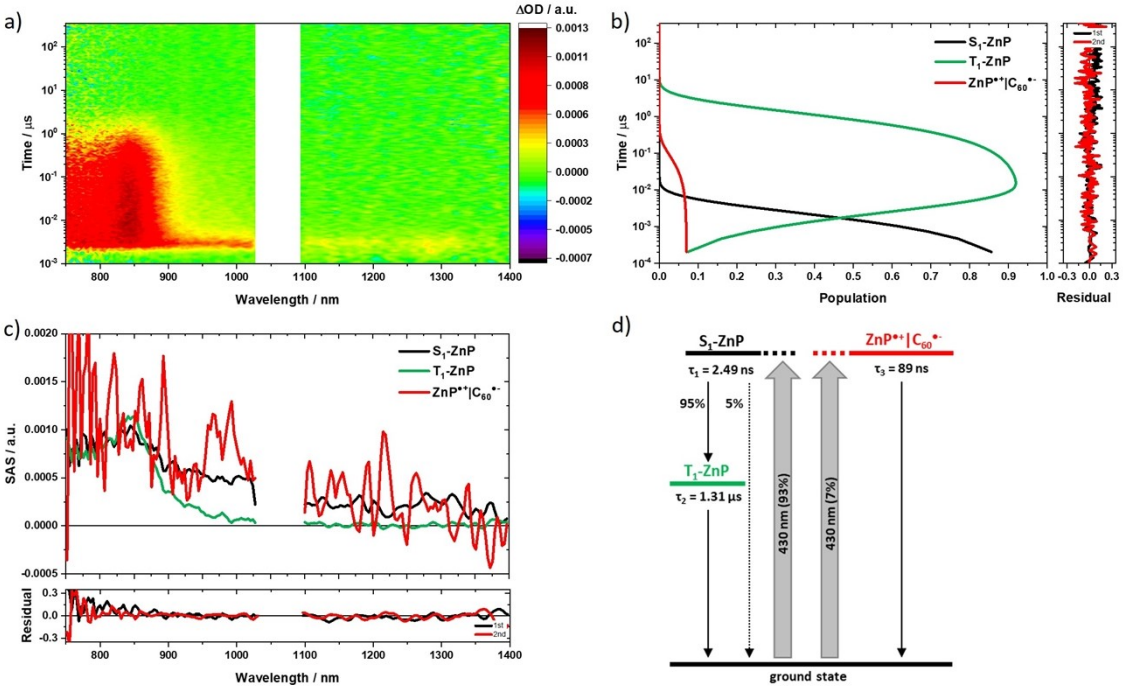

Fig. S9 a) Differential absorption spectra obtained upon nanosecond pump-probe experiments (430 nm) of a solution containing **ZnP** (c = 1 x 10^{-5} M) and $\mathbf{C_{60}}$ (c = 2 x 10^{-5} M) in anisole with several time delays between 0 and 400 µs. b) Population over time and c) SAS obtained upon chirp corrected GloTarAn analysis of the raw data with $\mathbf{S_1}$**-ZnP** (black), $\mathbf{T_1}$**-ZnP** (green), $\mathbf{ZnP^{\bullet+}|C_{60}^{\bullet-}}$ (red), and corresponding first (black) and second (red) singular vectors of the residual on the right (for b) and bottom (for c). d) Mechanistic model applied in GloTarAn. Relative energies are arbitrary in favor of clarity.

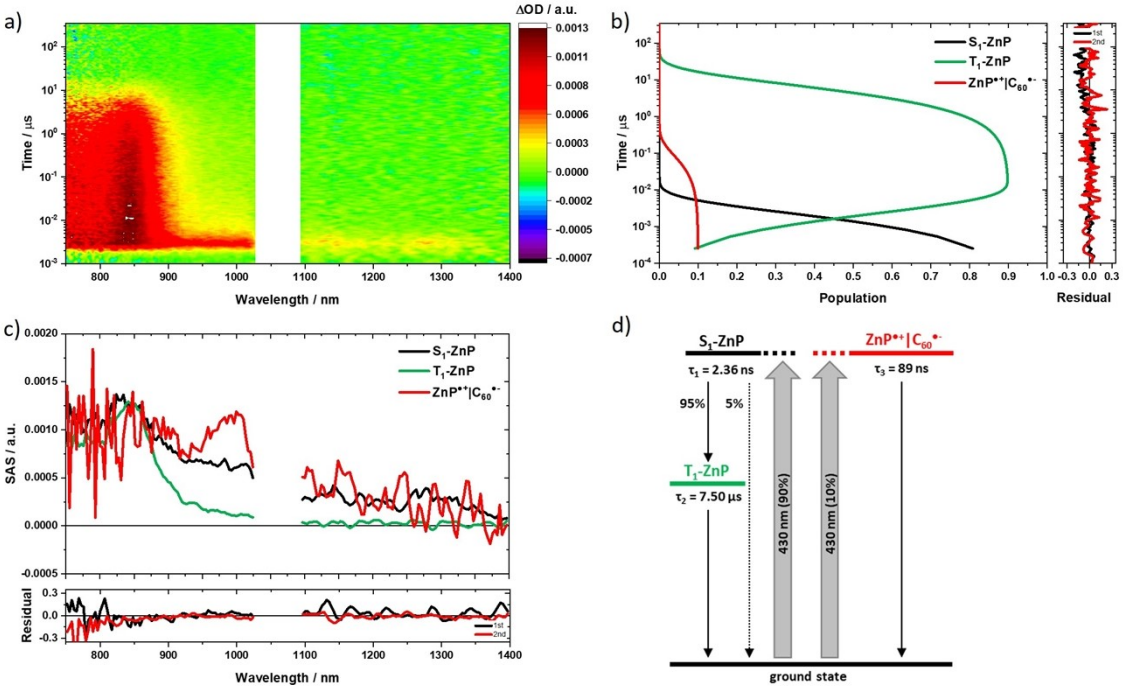

Fig. S10 a) Differential absorption spectra obtained upon nanosecond pump-probe experiments (430 nm) of a solution containing **ZnP** (c = 1 x 10^{-5} M) and $\mathbf{C_{60}}$ (c = 3 x 10^{-5} M) in anisole with several time delays between 0 and 400 µs. b) Population over time and c) SAS obtained upon chirp corrected GloTarAn analysis of the raw data with $\mathbf{S_1}$**-ZnP** (black), $\mathbf{T_1}$**-ZnP** (green), $\mathbf{ZnP^{\bullet+}|C_{60}^{\bullet-}}$ (red), and corresponding first (black) and second (red) singular vectors of the residual on the right (for b) and bottom (for c). d) Mechanistic model applied in GloTarAn. Relative energies are arbitrary in favor of clarity.

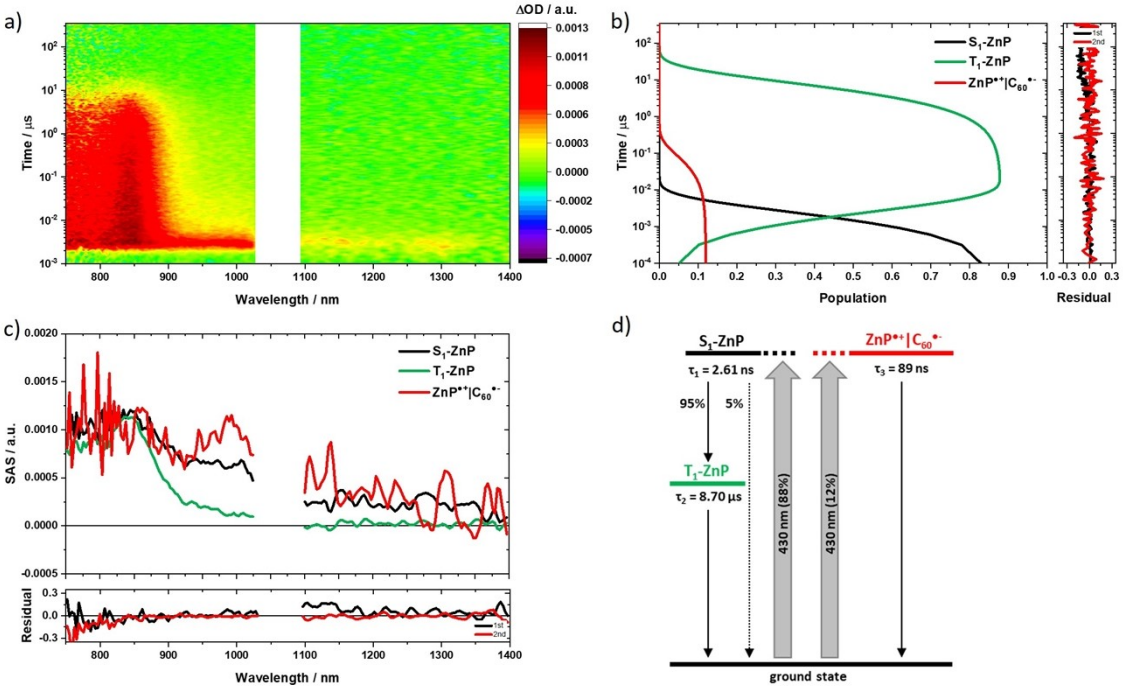

Fig. S11 a) Differential absorption spectra obtained upon nanosecond pump-probe experiments (430 nm) of a solution containing **ZnP** (c = 1 x 10^{-5} M) and $\mathbf{C_{60}}$ (c = 4 x 10^{-5} M) in anisole with several time delays between 0 and 400 µs. b) Population over time and c) SAS obtained upon chirp corrected GloTarAn analysis of the raw data with $\mathbf{S_1}$**-ZnP** (black), $\mathbf{T_1}$**-ZnP** (green), $\mathbf{ZnP^{\bullet+}|C_{60}^{\bullet-}}$ (red), and corresponding first (black) and second (red) singular vectors of the residual on the right (for b) and bottom (for c). d) Mechanistic model applied in GloTarAn. Relative energies are arbitrary in favor of clarity.

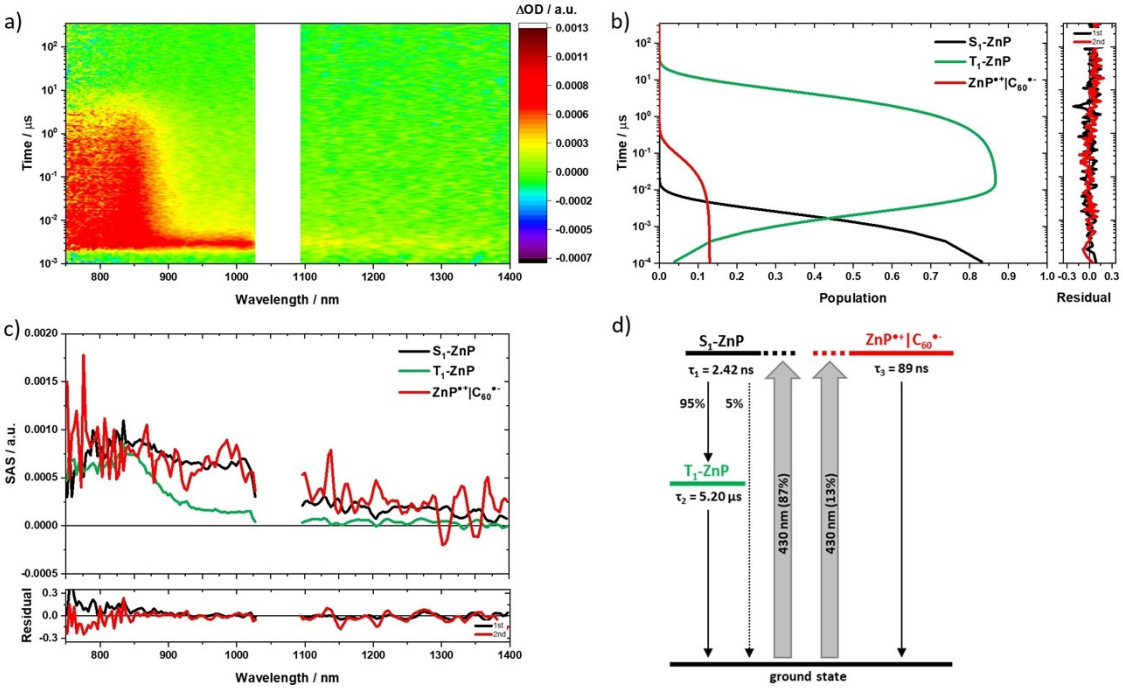

Fig. S12 a) Differential absorption spectra obtained upon nanosecond pump-probe experiments (430 nm) of a solution containing **ZnP** (c = 1 x 10^{-5} M) and $\mathbf{C_{60}}$ (c = 5 x 10^{-5} M) in anisole with several time delays between 0 and 400 µs. b) Population over time and c) SAS obtained upon chirp corrected GloTarAn analysis of the raw data with $\mathbf{S_1}$**-ZnP** (black), $\mathbf{T_1}$**-ZnP** (green), $\mathbf{ZnP^{\bullet+}|C_{60}^{\bullet-}}$ (red), and corresponding first (black) and second (red) singular vectors of the residual on the right (for b) and bottom (for c). d) Mechanistic model applied in GloTarAn. Relative energies are arbitrary in favor of clarity.

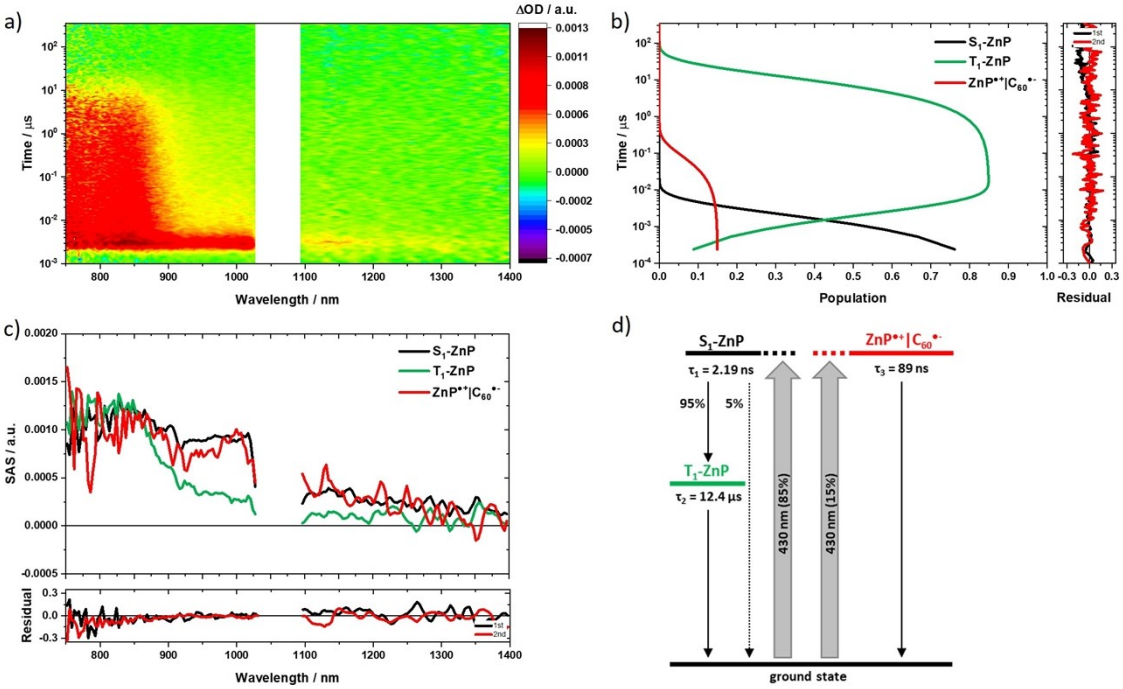

Fig. S13 a) Differential absorption spectra obtained upon nanosecond pump-probe experiments (430 nm) of a solution containing **ZnP** (c = 1 x 10^{-5} M) and $\mathbf{C_{60}}$ (c = 8 x 10^{-5} M) in anisole with several time delays between 0 and 400 µs. b) Population over time and c) SAS obtained upon chirp corrected GloTarAn analysis of the raw data with $\mathbf{S_1}$**-ZnP** (black), $\mathbf{T_1}$**-ZnP** (green), $\mathbf{ZnP^{\bullet+}|C_{60}^{\bullet-}}$ (red), and corresponding first (black) and second (red) singular vectors of the residual on the right (for b) and bottom (for c). d) Mechanistic model applied in GloTarAn. Relative energies are arbitrary in favor of clarity.

1 S. Kolemen, O. A. Bozdemir, Y. Cakmak, G. Barin, S. Erten-Ela, M. Marszalek, J.-H. Yum, S. M. Zakeeruddin, M. K. Nazeeruddin, M. Grätzel and E. U. Akkaya, *Chem. Sci.*, 2011, **2**, 949.

2 P. Rothemund and A. R. Menotti, *J. Am. Chem. Soc.*, 1948, **70**, 1808–1812.

3 C. Stangel, C. Schubert, S. Kuhri, G. Rotas, J. T. Margraf, E. Regulska, T. Clark, T. Torres, N. Tagmatarchis, A. G. Coutsolelos and D. M. Guldi, *Nanoscale*, 2015, **7**, 2597–2608.